isvr Institute of Sound and Vibration Research

Studies into the Detection of Buried Objects (Particularly Optical Fibres) in Saturated Sediment. Part 3: Experimental Investigation of Acoustic Penetration of Saturated Sediment

R.C.P. Evans and T.G. Leighton

ISVR Technical Report No 311

April 2007

University of Southampton

SCIENTIFIC PUBLICATIONS BY THE ISVR

Technical Reports are published to promote timely dissemination of research results by ISVR personnel. This medium permits more detailed presentation than is usually acceptable for scientific journals. Responsibility for both the content and any opinions expressed rests entirely with the author(s).

Technical Memoranda are produced to enable the early or preliminary release of information by ISVR personnel where such release is deemed to the appropriate. Information contained in these memoranda may be incomplete, or form part of a continuing programme; this should be borne in mind when using or quoting from these documents.

Contract Reports are produced to record the results of scientific work carried out for sponsors, under contract. The ISVR treats these reports as confidential to sponsors and does not make them available for general circulation. Individual sponsors may, however, authorize subsequent release of the material.

Studies into the detection of buried objects (particularly optical fibres) in saturated sediment. Part 3: Experimental investigation of acoustic penetration of saturated sediment.

R C P Evans and T G Leighton

ISVR Technical Report No. 311

April 2007

UNIVERSITY OF SOUTHAMPTON

INSTITUTE OF SOUND AND VIBRATION RESEARCH

FLUID DYNAMICS AND ACOUSTICS GROUP

Studies into the detection of buried objects (particularly optical fibres) in saturated sediment. Part 3: Experimental investigation of acoustic penetration of saturated sediment.

by

R C P Evans and T G Leighton

ISVR Technical Report No. 311

April 2007

Authorized for issue by
Professor R J Astley, Group Chairman

ACKNOWLEDGEMENTS

TGL is grateful to the Engineering and Physical Sciences Research Council and Cable & Wireless for providing a studentship for RCPE to conduct this project.

CONTENTS

ACKNOWLEDGEMENTS ii
CONTENTS iii
FIGURE CAPTIONS iv
ABSTRACT v
LIST OF SYMBOLS vi

1 INTRODUCTION 1

2 HISTORICAL 2

3 THE BIOT-STOLL THEORY 6

4 WAVE SCATTERING FROM ROUGH SURFACES 10

4.1 The Rayleigh Criterion 12

4.2 Random Rough Surfaces 14
4.2.1 Height Probability Distribution 14
4.2.2 Surface Correlations 15

4.3 Kirchhoff Theory 16

4.4 Perturbation Theories 18

4.5 Summary for scattering theory 19

5 ANOMALOUS ACOUSTIC PENETRATION 20

6 SUMMARY 28

REFERENCES 29

FIGURE CAPTIONS

Table 1 *Summary of the basic physical parameters required by the Biot-Stoll model.* 7

Figure 1 *The general, two-dimensional scattering geometry for fluid-borne acoustic waves incident on a rough, elastic boundary.* 13

Table 2 *Biot model parameters that have been applied to various grades of water-saturated sandy sediments.* 22

Figure 2 *Wave speeds as a function of frequency using the parameters shown in table 2 (computed using the OASES program). The curves correspond to the parameters of: Chotiros (black, solid) [1]; Stoll and Kan (blue, solid) [12]; Hovem and Ingram (red, solid) [25]; Stern et al (black, dotted) [50]; Ogushwitz (red, dotted) [54]; and Turgut and Yamamoto (blue, dotted) [55].* 23

Figure 3 *Pressure fields calculated above and below a water-sediment interface using the exact integral equation method: (a) flat surface; and (b) rough surface. The incident field comes from the left at a grazing angle of 20° and the critical angle is 27.8°. (This figure was reproduced from [60] with the permission of E I Thorsos.)* 26

ABSTRACT

This report is the third in a series of five, designed to investigate the detection of targets buried in saturated sediment, primarily through acoustical or acoustics-related methods. Although steel targets are included for comparison, the major interest is in targets (polyethylene cylinders and optical fibres) which have a poor acoustic impedance mismatch with the host sediment. This particular report provides a brief historical overview of sediment propagation models has been presented. Two theories have been covered: the Biot-Stoll theory; and wave scattering from random rough surfaces. The debate surrounding the observations of, so-called, anomalous acoustic penetration has also been discussed.

This series of reports is written in support of the article "The detection by sonar of difficult targets (including centimetre-scale plastic objects and optical fibres) buried in saturated sediment" by T G Leighton and R C P Evans, written for a Special Issue of *Applied Acoustics* which contains articles on the topic of the detection of objects buried in marine sediment. Further support material can be found at http://www.isvr.soton.ac.uk/FDAG/uaua/target_in_sand.HTM.

LIST OF SYMBOLS

a_{np}	Attenuation coefficient
a_p	Pore size parameter
c	Complex sound speed
c_p	Phase speed
C(**R**)	Surface height correlation function
d	Diameter of a sphere, or specifically of sediment grains
e	Exponential constant (~2.71828182)
f	Frequency
f(…)	Function of (…) in equation (21)
$G(\mathbf{r}, \mathbf{r}_0)$	Full-space acoustic Green's function
h_s	Surface height above a reference plane
h_1	Height above the reference plane of the scattering point on a rough surface which is located at horizontal coordinate x_1
h_2	Height above the reference plane of the scattering point on a rough surface which is located at horizontal coordinate x_2
Δh_s	Difference in height between two scattering points on a rough surface (i.e. $\Delta h_s = h_1 - h_2$)
i	Complex operator, $\sqrt{-1}$
k	Wave number modulus
k	Complex wave number
K	An empirically-derived constant

K_b	Bulk modulus
$\overline{K}_b$	Complex bulk modulus of a sediment's skeletal frame
K_{bi}	Imaginary component of the complex bulk modulus of a sediment's skeletal frame
K_{br}	Real component of the complex bulk modulus of a sediment's skeletal frame
k_f	Permeability
K_f	Bulk modulus of pore fluid
K_r	Bulk modulus of sediment grains
$\mathbf{n}_0$	The unit surface normal at $\mathbf{r}_0$, pointing towards an acoustic source
$p(h_s)$	Statistical height distribution, such that $p(h_s)dh_s$ is the probability of any surface point being between h_s and $(h_s+ dh_s)$ above the reference plane
Q_a	Quality factor
Q_a^{-1}	Specific attenuation factor
r	Radial distance from a scattering centre
$\mathbf{r}$	The position vector of the point of interest on a reference surface
R	A general co-ordinate point
$\mathbf{R}$	Vector separating two surface points
$\mathbf{r}_0$	Co-ordinate vector of a point on a rough surface
R_a	Rayleigh parameter
R_{dB}	Reflection loss
$\mathbf{R}_{Pa}$	Complex reflection coefficient
S_0	Surface area per unit volume of the particles in the sediment
$\mathbf{S}_0$	Vector describing a scattering surface
t	Time
v_p	Phase velocity

x	Cartesian co-ordinate in the horizontal plane
x_1	Horizontal co-ordinate position of a scattering point on a rough surface
x_2	Horizontal co-ordinate position of a scattering point on a rough surface
y	Cartesian co-ordinate in the horizontal plane
z	Cartesian co-ordinate in the vertical plane
α_{dB}	Attenuation coefficient
α_s	Structure factor
β	Porosity
δ	Logarithmic decrement
δ_p	Sediment frame longitudinal wave log decrement
δ_s	Sediment frame shear log decrement
η_f	Viscosity of pore fluid
λ_0	Correlation length
$\bar{\mu}$	Complex shear modulus of sediment skeletal frame
μ_i	Imaginary component of the complex shear modulus of sediment skeletal frame
μ_r	Real component of the complex shear modulus of sediment skeletal frame
π	Pi (≈ 3.141592654)
θ_L	Effective loss angle
θ_1	Angle of incidence for plane monochromatic wave incident onto a rough surface

θ_2	Angle, measured with respect to the normal of the reference plane, of a ray scattered into the azimuthal plane from a rough surface.
$\Delta\theta$	Phase difference between two rays scattered from separate points on a rough surface
ρ_f	Density of a fluid
ρ_r	Density of a sediment grain
σ	Poisson's ratio of the frame
σ_h	Surface height rms deviation of a rough surface from a reference plane
ω	Circular frequency
ψ	Acoustic scaler wave potential
ψ_i	Incident acoustic scaler wave potential
ψ_s	Scattered acoustic scaler wave potential
∇	Differential operator $\left(\frac{\partial}{\partial x}, \frac{\partial}{\partial y}, \frac{\partial}{\partial z}\right)$

1 Introduction

In order to investigate the possibilities for the detection of buried objects (particularly optical fibres) in saturated sediment[1], a test tank facility (with acoustic sensors) was set up, and investigations made into the acoustic properties of the water and the sediment material used[2]. This investigation included measurements of sound speed and attenuation. For the sediment in particular, reference was made to an empirical model for the attenuation of sound in the seabed (see section 2.2.4 of the second report in the series[2]). Measurements of attenuation in the laboratory sand were also presented. Transmission phenomena at the water-sediment interface were discussed in section 2.2.5 of the second report in the series[2], where it was noted that the assumption of a flat 'fluid-fluid' interface is often valid. It was also noted that the scattering of acoustic waves at a rough interface was an important issue that required further study.

The transmission of sound at a rough interface is a topic of particular academic interest following a recent debate where previous views on acoustic penetration were questioned. Historically, elastic sediment models have been considered adequate in the 10 - 100 kHz frequency range, the range of particular interest in this investigation. Snell's law states that no energy can penetrate into a sediment if it is incident below the critical grazing angle. However, recent measurements [1] have suggested anomalous acoustic penetration below the critical angle; a phenomenon that is inconsistent with existing models.

The propagation of shear waves is not considered in detail in this report since it is widely accepted that they are more highly attenuated in sediments than compressional waves. This makes them less suitable for the types of detection processing that are

---

[1] T G Leighton and R C P Evans, Studies into the detection of buried objects (particularly optical fibres) in saturated sediment. Part 1: Background. *ISVR Technical Report No.* 309 (2007).

[2] T G Leighton and R C P Evans, Studies into the detection of buried objects (particularly optical fibres) in saturated sediment. Part 2: Design and commissioning of test tank. *ISVR Technical Report No.* 310 (2007).

investigated in a subsequent report in this series[3]. Instead, the main focus of this current report is on the propagation of compressional waves within marine sediment. In the first section (section 2), a historical overview of sediment propagation models is presented. Two approaches have been considered in detail: The Biot-Stoll theory [2] is presented in section 3. This postulates the existence of a second compressional wave in addition to the ordinary compressional wave and shear wave. Rough surface scattering models are presented in section 4. It should be noted that roughness scattering is a large field of study that cannot be fully covered in this report. However, section 4 should give the reader some insight into the different approaches that have been taken, and the regimes of validity of the corresponding models.

The debate surrounding anomalous acoustic penetration is detailed in section 5. The conflicting explanations (the Biot-Stoll theory and rough surface scattering) are noted.

2 Historical

A comprehensive review of the mechanisms affecting the propagation of acoustic waves in the seabed has been performed by Kibblewhite [3]. In this article it is noted that in both shallow and deep water environments, the seabed is often the dominant factor controlling propagation. An acoustically 'lossy' seabed causes attenuation of sound through compressional-wave absorption in the bottom and the excitation of shear waves.

On the basis of extensive experimental evidence, Hamilton has argued that attenuation is linearly related to frequency over the whole range of frequencies encountered in underwater acoustics (from a few hertz to megahertz, the so-called 'f^1 law') [4]. A subset of this evidence is presented in section 2.2.4 of the second report in the series[2], where it is established that a linear scaling law can be applied to the laboratory sand for the range of frequencies that are of interest in this investigation. However, the question of whether the attenuation in saturated, unconsolidated marine

[3] R C P Evans and T G Leighton, Studies into the detection of buried objects (particularly optical fibres) in saturated sediment. Part 4: Experimental investigations into the acoustic detection of objects buried in saturated sediment. *ISVR Technical Report No.* 312 (2007).

sediments is accurately proportional to frequency over an extended range is still under debate [5, 6].

When sound energy passes through a saturated sediment, energy is lost through a number of mechanisms. Some are fundamental to the material and are referred to as 'intrinsic attenuation'. These are internal friction at grain-to-grain contacts [4], which gives rise to a linear scaling with frequency, and viscous losses due to the relative motion of the pore fluid and the frame [7]. Frictional losses are large when rigidity is large since rigidity depends on inter-particle contacts. The rigidity of sediments is a function of the fractional pore space. A comparison of the dependence of the attenuation constant on porosity and rigidity confirms this relationship [8]. The additional viscous loss components are responsible for any deviation from the f^1 law in saturated sediments.

Other factors can play a part in the attenuation process in the seabed, such as trapped gas bubbles and inhomogeneities that produce losses through scattering. (The presence of gas bubbles in the sediment is considered in section 2.1.1 of the second report in the series[2], and a process is described to actively remove bubbles from the laboratory sand.) At high frequencies, where the wavelength of sound waves is close to the size of individual grains, scattering is the dominant loss mechanism. Energy conversion between compressional, shear and interface waves also leads to significant attenuation. The total of all these losses is referred to as the 'effective attenuation'.

Several theories of attenuation in granular materials have been explored over the years. In one approach, the sediment medium is considered to be a continuum with visco-elastic properties that are representative of the bulk material as a whole [3]. The acoustic response is then described by complex moduli and relaxation functions that are adjusted to give results consistent with real materials. Consider, for example, the Hamilton visco-elastic model. This assumes that sediments can be represented by an isotropic two-phase system composed of sediment grains and water [9]. Provision is made for velocity dispersion and a non-linear dependence of attenuation on frequency. The model leads to an equation for both the shear and compressional attenuation which is of the form:

$$Q_a^{-1} = \frac{a_{np} v_p}{\left(\pi f - a_{np}^2 v_p^2 / 4\pi f\right)} \tag{1}$$

where Q_a^{-1} is the specific attenuation factor, a_{np} is the attenuation coefficient, v_p is the phase velocity and $f = \omega/2\pi$ is the frequency. It is also common to use the attenuation coefficient, $\alpha_{dB} = a_{np} \times 20 \log_{10} e$, having units of decibels per unit length.

When energy losses are small, the term $a_{np}^2 v_p^2 / 4\pi f$ can be ignored. Thus, equation 1 can be reduced to the following:

$$Q_a^{-1} = \frac{a_{np} v_p}{\pi f} = \frac{2 a_{np} v_p}{\omega} = \frac{\delta}{\pi} = \tan\theta_L \tag{2}$$

where δ is the logarithmic decrement, the natural logarithm of the ratio of the amplitudes of two successive cycles of an exponentially decaying sine wave. The parameter θ_L is the effective loss angle. In acoustics, this is equivalent to the phase difference between stress and strain under harmonic loading. The wave velocities, specific attenuation factor and logarithmic decrement are independent of frequency if the attenuation coefficient is proportional to the first power of frequency [9].

An alternative to the visco-elastic model approach assumes that wave propagation depends on the properties of individual constituents of the material and on the structural characteristics of the skeletal frame. This may be described as a physical model approach.

The Biot model fits into the category of physical sediment models [10, 11]. According to the theory, sound energy is transported through the fluid and the frame by two compressional waves and a shear wave. This results in a frictional loss attenuation that is proportional to frequency, f, and a viscous attenuation that varies from f^2 at low frequencies to $f^{1/2}$ at higher frequencies. (The viscous loss is introduced by allowing for the relative motion between the frame and pore fluid.)

Stoll later extended Biot's theoretical developments by treating the shear and bulk moduli of the skeletal frame as complex quantities [12, 13]. The model predicts slight velocity dispersion and a non-linear relationship between attenuation and frequency. However, there are some difficulties associated with the Biot-Stoll theory:

- It does not account for the characteristic attenuation exhibited by granular materials over an extended frequency range.
- The effect of a distribution of grain sizes in the sediment cannot easily be taken into account.
- It is only valid for sands composed of uniformly spherical grains, such that porosity is independent of grain size.

The Biot-Stoll theory may be considered too simple to be applied to real sediments. However, by careful selection of parameters, the attenuation losses predicted by the theory can be made to fit most experimental data [7]. Exceptions to this are muddy sediments which have porosities that are, typically, between 60 % and 85 %. Such large porosities suggest that the particles are suspended in a fluid matrix rather than packed into a rigid skeletal frame. Sediments of this kind must be treated as fluids, rather than as Biot media, requiring the use of multiple scattering models [14]. The Biot-Stoll theory is considered in more detail in section 3.

An entirely different model of acoustic propagation in saturated, unconsolidated, marine sediments has recently been proposed by Buckingham [5, 6, 15]. It is developed on the basis of a linear wave equation which includes a dissipation term representing the losses that arise from inter-particle contacts. This loss term takes into account the hysteresis (or 'memory') exhibited by granular media, by setting the frictional stress at inter-particle contacts equal to a temporal convolution between particle velocity and a material memory function.

Two equations emerge from the analysis: one for compressional wave propagation; and the other for shear wave propagation. The compressional wave shows an attenuation that scales almost exactly with the first power of frequency, and a weak logarithmic dispersion in phase velocity. The shear equation admits a wave-like solution even though the sediment shows no elastic rigidity. The shear wave also shows an attenuation that scales as f^1. When combined with a model of the mechanical properties of marine sediments, the compressional and shear wave speeds can be related to the grain size, porosity and density of the medium. Buckingham states that this analysis show close agreement with the observed geo-acoustic properties of many unconsolidated marine sediments.

A full description of the behaviour of marine sediments must also include interface waves at the seawater-sediment boundary [16]. Surface waves are known to exist in unconsolidated sediments and are sometimes used as an indirect means of determining the speed of shear waves. Sediments are often assumed to behave like elastic solids, in which case the interface waves are of the Stonely, or Scholte, type with speeds that are 80 - 90 % of the shear wave speed [17]. This type of wave process occurs at the interface between elastic and fluid half-spaces, and is concentrated in a layer of thickness of the order of a wavelength in the fluid [18]. In Buckingham's new theory of acoustic propagation in marine sediments, a pseudo-Scholte wave is shown to propagate with a speed that is in agreement with experimental measurements [17].

Surface roughness is also an important factor in determining the behaviour of acoustic waves incident on the seawater-sediment boundary, or on internal interfaces between sediment layers. The scattering process depends on the wavelength of the incident radiation and the degree of roughness of the interface, as determined by statistical techniques. (Since all real surfaces are rough and no two rough surfaces are identical, statistical techniques are usually required to describe them.) The topic of acoustic wave scattering from rough surfaces is considered in more detail in section 4.

3 The Biot-Stoll Theory

Biot developed a comprehensive theory for the static and dynamic response of porous materials containing compressible fluid. He considered both low and high frequency behaviour and included the possibility of visco-elastic or visco-dynamic response in various components of his model. An abbreviated derivation leading to one form of the Biot equations is given by Stoll [2]. This derivation helps to identify the variables that are used, and to visualise how the response of the sediment is modelled in a mathematical way.

Biot's theory predicts that, in the absence of boundaries, three kinds of body waves may exist: two compressional (dilatational) and one shear (rotational), in a fluid-saturated, porous medium. One of the compressional waves (the 'first kind') and the shear wave are similar to waves found in ordinary elastic media. The motions of the skeletal frame and the interstitial fluid are nearly in phase and the attenuation owing

to viscous losses is relatively small. In contrast, the compressional wave of the 'second kind' is highly attenuated, with the frame and fluid components moving largely out of phase.

Compressional waves of the second kind become important in acoustical problems involving very compressible pore fluids (such as air). However, waves of the first kind are of principal interest in water-saturated sediments. A possible exception to this can occur in the case of a very gassy sediment where the effective compressibility of the pore fluid is greatly reduced by the presence of free or dissolved gasses [19, 20].

In order to determine the velocity and attenuation in real sediments, it is necessary to choose realistic values for the physical parameters summarised in table 1. Following Stoll's example, these can be divided into three groups: bulk; fluid motion; and frame response. Several of the choices are straightforward. However, a few of the parameters require careful consideration in order to produce meaningful predictions [1, 21].

Frequency-independent variables	
Porosity	β
Mass density of grains	ρ_r
Mass density of pore fluid	ρ_f
Bulk modulus of sediment grains	K_r
Bulk modulus of pore fluid	K_f
Variables affecting global fluid motion	
Permeability	k_f
Viscosity of pore fluid	η_f
Pore size parameter	a_p
Structure factor	α_s
Variables controlling frequency-dependent response of frame	
Shear modulus of skeletal frame	$\overline{\mu} = \mu_r(\omega) + i\mu_i(\omega)$
Bulk modulus of skeletal frame	$\overline{K}_b = K_{br}(\omega) + iK_{bi}(\omega)$

Table 1 *Summary of the basic physical parameters required by the Biot-Stoll model.*

The bulk parameters are the simplest to obtain. There may be slight variations in the values of the density and the bulk modulus of the pore fluid, but these are generally insignificant. The grain density can be measured from sediment samples. It is only the grain bulk modulus that can be difficult to measure because of the small size of the sediment grains.

The fluid motion parameters can be difficult to determine. It is only the viscosity that is relatively simple to measure, whereas permeability can be much harder to obtain (especially for sediments containing flocculant particles such as silt and clay). Permeability can be determined from empirical relationships based on porosity and grain size [9, 22, 23], or through physical relationships such as the Kozeny-Carman equation [24]:

$$k_f = \frac{1}{KS_0^2}\left(\frac{\beta^3}{(1-\beta)^2}\right) \tag{3}$$

where K is an empirical constant, approximately equal to 5, and S_0 is the surface area per unit volume of the particles in the sediment. The value of S_0 is defined for a sphere as $S_0 = 6/d$ where d is the diameter. However, to be realistic the value of S_0 must be modified to account for the fact that natural sediments are not spherical and do not have uniform-sized grain diameters.

The pore size parameter was introduced by Biot to describe the dependence of the viscous resistance to fluid flow on the size and shape of the pore. With appropriate values for the pore size parameter, the equations of motion for cylindrical pores can be applied to other pore geometries. Hovem and Ingram [25] defined it as being twice the 'hydraulic radius', which is the ratio of the volume of pore fluid to the area of the wetted surface. The hydraulic radius concept is applicable to any porous medium with interconnected pores. Hence, the pore size parameter can be determined through the Kozeny-Carman relation following Hovem and Ingram:

$$a_p = 2\sqrt{\frac{Kk_f}{\beta}} \tag{4}$$

where K represents the same empirical constant as in equation (3).

The structure factor α_s (also referred to as the 'virtual mass coefficient') is a dimensionless term introduced in the Biot-Stoll theory to account for the transfer of momentum from the fluid to the frame. It increases with the 'tortuosity' of the pore spaces, theoretically varying from a value of 1.0 for uniform pores to a value of 3.0 for a random system of pores. In practice, the structure factor is determined experimentally.

In modelling the coarser, granular materials the moduli $\overline{K}_b$ and $\overline{\mu}$ are chosen to be complex constants. The ratios of their imaginary to real parts are determined on the basis of experimental measurements. The frame shear modulus is rarely obtained by direct measurement. Its real part can be calculated by the use of empirical relations. The imaginary part is descriptive of losses at grain-to-grain contacts and is related to the attenuation of shear waves. Its value can be obtained through the following relationship:

$$\mu_i = \frac{\mu_r \delta_s}{\pi} \tag{5}$$

where μ_r is the real part of the frame shear modulus. The frame shear log decrement, δ_s, is a measure of the shear wave attenuation coefficient and is computed from shear wave attenuation measurements.

The frame bulk modulus is the most difficult parameter to determine. There is no satisfactory method of direct measurement. It can be determined from the frame shear modulus using the standard elastic relationship for solids:

$$K_{br} = \frac{2}{3}\left(\frac{1+\sigma}{1-2\sigma}\right)\mu_r \tag{6}$$

where σ is the Poisson's ratio of the frame.

The imaginary part of the frame bulk modulus is descriptive of losses at grain-to-grain contacts and is related to the attenuation of compressional waves. Its value can be determined by the log decrement of longitudinal waves, δ_p, which is analogous to the frame shear log decrement.

It may be assumed that the wave amplitude and the logarithmic decrement are small so that different measures of damping may be related in a simple way. For example,

the quality factor, Q_a, the logarithmic decrement, δ, (for both travelling waves and stationary vibrations) and the attenuation coefficient, α_{dB}, may be related using equation (2), above.

As noted in section 1, the Biot-Stoll theory has been used by certain authors as a means of explaining measurements of anomalous acoustic penetration of the seabed at sub-critical grazing angles. The measurements, and the issues surrounding the manner in which the theory was applied, are presented in section 5.

4 Wave Scattering from Rough Surfaces

There have been numerous attempts to model acoustic wave scattering from rough surfaces over the years. For example, Patterson derived a semi-empirical model [26] based on acoustic scattering data that assumed specular and sidelobe scattering from planar facets of the seawater-sediment boundary. An alternative technique was later developed that enabled the Helmholtz-Kirchhoff integral to be evaluated over the scattering interface [27]. It was assumed that the reflection coefficient was constant, and that multiple scattering between irregularities was negligible.

A similar approach has been applied using a 'composite roughness model' [28] to account for surfaces that are rough on scales both large and small relative to the radiation wavelength. Large-scale roughness is treated as a random slope variation using the Kirchhoff approximation, and small-scale roughness is treated by a perturbation method [29]. Although composite roughness models are useful, their results depend on the way in which the scale of the surface roughness is partitioned, and they are inaccurate for scattering at low grazing angles. Therefore there has been much interest in developing a unified approach that spans both the Kirchhoff approximation and the small perturbation regimes [30].

The importance of scattering from below the sediment interface was suggested after experiments involving measurements of scattering from a rippled, sandy surface [31]. A strong dependence of the scattering strength on azimuthal orientation was expected but was *not* observed. This was taken as evidence of volume scattering from below the interface. A significant contribution to volume scattering in real sediments is made by trapped gas bubbles. Since this is mentioned elsewhere in this study (see section

2.1.1 of the second report in the series[2]) it will not be considered further here, other than to note that bubbles in resonance are very strong scatterers of sound.

It is usual to consider the problem of scattering separately for surface roughness and volume reverberation [32]. However, the contributions to the total scattered field from these two types of irregularity are difficult to separate. Experimental measurements have failed to provide conclusive evidence to determine whether volume or interface scattering is the dominant effect [29, 33]. More recently, researchers have begun to show interest in a unified approach to surface roughness and volume reverberation scattering based on small volume perturbations [32, 34]. In this case, roughness can be considered as a specific kind of volume perturbation near the mean, flat interface.

The following sections follow the approach to scattering from random rough surfaces taken by Ogilvy [35]. (This approach mainly deals with the back-scattering of acoustic energy into the water column. However, the back-scattering of incident energy is necessarily paired with the transmission and conversion of energy into the sediment [36].) Scattering from surfaces where the dominant roughness is periodic is also considered. This is a separate topic to scattering from random surfaces, where techniques can be used that exploit the periodicity of the scatterer. Such surfaces give rise to 'grating modes', *i.e.*, energy scattered strongly into specific directions that are determined by the wavelength of the periodicity compared with the wavelength of the incident wave [35].

Periodic rough, or 'rippled', sediment surfaces occur naturally as a result of the flow of water at the water-sediment interface [37]. Ripples are better described as a series of corrugations that are, typically, spaced a few centimetres apart. In plan view, ripple patterns show considerable variety. There is a tendency for straight ripples to form in deep water or at low current speeds, and for more complicated, three-dimensional ripples to form in shallower water and higher speeds.

In the study of cables buried at a typical sea depth of 1 000 m, and at frequencies in the 10 - 100 kHz range, scattering from sediment grains (having a length-scale ~ mm) is of greater importance than scattering from ripples (having a length-scale ~ cm). This is because, typically, the deep sea floor is a tranquil environment. Only certain areas are known to be affected by currents that are strong enough to rework the bottom sediment and create ripple patterns [38]. It should be noted that the sand used

in the laboratory tank was chosen on the basis that it was similar to the sediment material at the sea depth of interest.

An experiment is described in reference [61], in which scattering was measured for both small-scale, and large-scale, roughness over the surface of the sediment in the laboratory tank. In that experiment, the granular roughness was similar to that found over the surface of a naturally-occurring 'medium' sand, according to the Wentworth grain size classification [39]. (It should be noted that the particle size distribution measurement, presented in section 2.1.2 of the second report in the series[2], showed that the sediment material was a 'very fine sand'. This discrepancy arises from the uncertainty associated with the height variation measurement in the experiment). The large-scale roughness was more representative of the 'worst-case' that could be expected to occur naturally in the field.

A similar experiment is documented in the literature [40]. Pace and Ceen conducted a series of measurements of the spatial dependence of waveforms generated by water-borne parametric arrays. In these measurements, the source volume was truncated by a water / sand interface. The results consisted of the acoustic signals received on a hydrophone buried in the sand. It was noted that when the water / sand interface was sinusoidal there existed the possibility that a range of signals would arrive at the receiver. This was, in fact, observed to be the case; several additional directive sources, which were described as being multiple images of the directive source located at the transducer, were recorded at the hydrophone. It was also suggested that when the interface was non-planar, more acoustic energy would reach the sand-borne hydrophone than when it was plane.

4.1 The Rayleigh Criterion

Wave scattering from real, rough surfaces was first studied by Rayleigh who considered the problem of a plane monochromatic wave incident normally onto a sinusoidal surface. This work led to the development of the 'Rayleigh criterion' for determining the degree of roughness of a surface [41].

Consider a plane monochromatic wave incident at some angle, θ_1, onto a rough surface. For waves scattered into the azimuthal plane at some angle, θ_2, the phase difference between two rays scattered from separate points on the surface is given by

$$\Delta\theta = k\left[\left(h_1 - h_2\right)\left(\cos\theta_1 + \cos\theta_2\right) + \left(x_2 - x_1\right)\left(\sin\theta_1 - \sin\theta_2\right)\right] \tag{7}$$

where k is the modulus of the incident (and scattered) wave vector and the scattering points are located at x_1 and x_2.

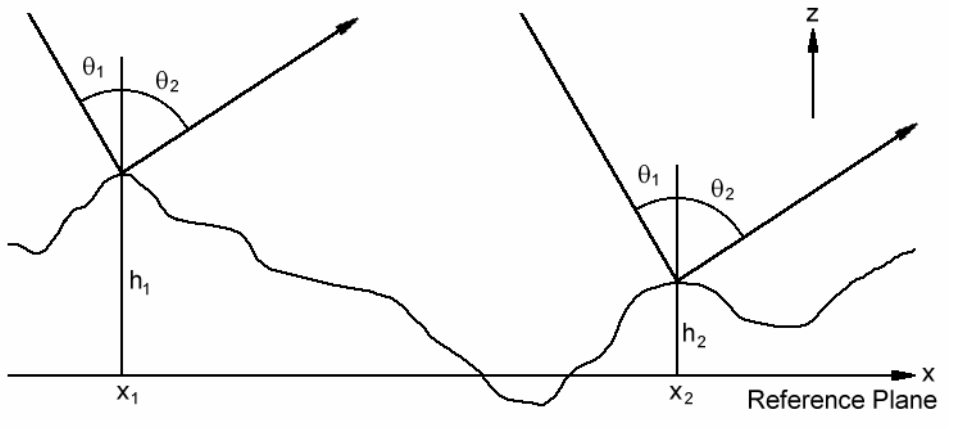

Figure 1 *The general, two-dimensional scattering geometry for fluid-borne acoustic waves incident on a rough, elastic boundary.*

The heights of the scattering points relative to the reference plane are h_1 and h_2. For specular scattering ($\theta_1 = \theta_2$) the phase difference becomes

$$\Delta\theta = 2k\Delta h_s \cos\theta_1 \tag{8}$$

where $\Delta h_s = h_1 - h_2$. The interference between these rays depends on the magnitude of the phase difference compared with π. For $\Delta\theta << \pi$ the two waves will be almost in phase and will constructively interfere. However, for $\Delta\theta \sim \pi$ the waves will destructively interfere, leading to no contribution to the scattered energy in the specular direction. The 'Rayleigh criterion' states that if $\Delta\theta < \pi/2$ then the surface is smooth rather than rough. If this restriction is averaged across a surface then Δh may be replaced by σ_h, where this is the surface rms deviation from the reference plane, and the criterion becomes

$$R_a < \frac{\pi}{4} \tag{9}$$

where R_a, known as the 'Rayleigh parameter' [41], is given by

$$R_a = k\sigma_h \cos\theta_1 \tag{10}$$

The Rayleigh criterion for dividing surfaces into 'rough' or 'smooth' is quite arbitrary. However, it does illustrate the point that the roughness of any scattering surface is not an intrinsic property of that surface, but depends on the properties of the wave being scattered. Both the *frequency* and *angle* of the incident wave determine how rough any surface appears to be. A surface appears to be rougher the smaller the incident wavelength, or the closer the angle of incidence is to surface normal.

4.2 Random Rough Surfaces

A rough surface is usually described in terms of its deviation from a smooth reference surface [42]. The shape and location of the reference surface are chosen according to the long-range behaviour of the rough surface. For example, a description of a rough cylinder would involve measurements of height deviations from a cylindrical reference surface, whereas the profile of a rough sea would be measured from a flat reference plane.

There are, essentially, two aspects to the nature of a random rough surface: the spread of heights about the reference surface; and the variation of these heights along the surface. A variety of statistical distributions and parameters are used to describe these properties [35], including: the 'structure function', defined as the mean square of the difference in surface height; the 'characteristic function', defined as the Fourier transform of the height probability density function; and the power spectral density, defined as the Fourier transform of the surface covariance function. Higher order properties are also of interest [43], both in the theory of wave scattering from random rough surfaces and in the classification of measured surface profiles.

Surface height distribution and correlation functions are considered, below, as these are the surface functions that most commonly appear in theories of wave scattering.

4.2.1 Height Probability Distribution

The deviation of a surface from the smooth reference surface is represented here by the function $h_s(\mathbf{r})$, where h_s is the height of the surface from reference surface and $\mathbf{r}$ is

the position vector of the point of interest on the reference surface. The surface is thus assumed to be part of a continuous random process, h_s. The distribution of surface heights is described by the statistical height distribution $p(h_s)$, where $p(h_s)dh_s$ is the probability of any surface point being at a height between h_s and $h_s + dh_s$ away from the mean surface. It is usual to ensure that h satisfies

$$\langle h_s \rangle_s = \int_{-\infty}^{\infty} h_s p(h_s) dh_s \Big| = 0 \tag{11}$$

where $\langle ... \rangle_s$ denotes the process of spatial averaging, *i.e.*, averaging across the surface. This assumption has the advantage of simplifying most theories of wave scattering from rough surfaces. Measurements of surface profiles may always be adjusted to ensure equation (11) is satisfied by a suitable choice of the reference surface. The rms height of the surface is then equal to the standard deviation and is given by

$$\sigma_h = \sqrt{\langle h_s^2 \rangle|_s} \tag{12}$$

Much of the literature on rough surfaces assumes that height distributions are Gaussian. For a surface satisfying equation (11) the distribution is then given by

$$p(h_s) = \frac{1}{\sigma_h \sqrt{2\pi}} \exp\left(-\frac{h_s^2}{2\sigma_h^2} \right) \tag{13}$$

The distribution is symmetrical about zero, so that Gaussian surfaces have an equal number of surface points above and below the reference surface.

4.2.2 Surface Correlations

The specification of a height distribution and rms height does not discriminate between surfaces having different 'length scales', *i.e.*, the characteristic length over which height changes occur along the surface.

Such surfaces may be distinguished by their correlation functions, defined as

$$C(\mathbf{R}) = \frac{\langle h_s(\mathbf{r}) h_s(\mathbf{r}+\mathbf{R}) \rangle|_s}{\sigma_h^2} \tag{14}$$

As **R** increases, C(**R**) will usually decay to zero, with the shape of this decay being dependent on the type of surface and with the rate of decay being dependent on the

distance over which points become uncorrelated. This will not be true, however, for surfaces that are not truly random. For example, the correlation function of a sinusoidal surface takes the form of a cosine function, reflecting the periodic nature of the surface. Only if there is some finite distance over which the surface profile is truly uncorrelated will the correlation function decay to zero.

The theory of wave scattering from rough surfaces often assumes that surface correlation functions are Gaussian and may be given by

$$C(R) = \exp\left(-\frac{R^2}{\lambda_0^2}\right) \tag{15}$$

In equation (15), λ_0 is usually called the 'correlation length' [35], this being the distance over which the correlation function falls to 1/e. The spatial variable, **R**, has been replaced by R since the statistics of the surface are assumed to be independent of direction. (Anisotropy can be introduced into the statistical description of rough surfaces by using different correlation lengths in two perpendicular directions along the surface.)

4.3 Kirchhoff Theory

Kirchhoff theory (also known as tangent plane or physical optics theory) is the most widely used theory in the study of scattering from rough surfaces [44]. It provides an approximation to the wave field on the surface of a scatterer. Any point on a scatterer is treated as though it were part of an infinite plane, parallel to the local surface tangent. An integral formula is used to give an expression for the scattered field at some distance from a scatterer in terms of the approximated field surface. The integral formula depends on the nature of the wave field. The theory is exact for an infinite, smooth, plane scatterer.

The simplest form of Kirchhoff theory arises when a plane, monochromatic, scalar wave is incident onto a rough surface with a reflection coefficient that is independent of position along the surface. Complications may be added to the theory, such as varying surface reflection coefficients and finite-width beams, but only at the expense of the ease of solution.

Consider the field quantity, ψ, which represents a scalar wave potential. In the presence of a scatterer the total field $\psi(\mathbf{r})$ may be taken to be composed of the incident field $\psi_i(\mathbf{r})$ and a field arising from the interaction of the incident field with the scatterer, $\psi_s(\mathbf{r})$:

$$\psi(\mathbf{r}) = \psi_i(\mathbf{r}) + \psi_s(\mathbf{r}) \tag{16}$$

When the surface of the scatterer, $\mathbf{S}_0$, is closed (*i.e.*, the surface encloses a finite volume) then the total field at any point r is given exactly by the Helmholtz interior or exterior scattering formula [35]:

$$\psi(\mathbf{r}) = \psi_i(\mathbf{r}) + \int_{\mathbf{S}_0} \left[\psi_s(\mathbf{r}_0) \frac{\partial G(\mathbf{r},\mathbf{r}_0)}{\partial \mathbf{n}_0} - G(\mathbf{r},\mathbf{r}_0) \frac{\partial \psi_s(\mathbf{r}_0)}{\partial \mathbf{n}_0} \right] d\mathbf{S}_0 \tag{17}$$

where $\mathbf{r}$ is inside a closed volume containing no sources of $\psi_i(\mathbf{r})$ or $\psi_s(\mathbf{r})$ (interior formula) or outside a volume that contains all the field sources (exterior formula). In equation (17), integration is over $\mathbf{S}_0$ (the surface of the scatterer), $\mathbf{n}_0$ is the unit surface normal pointing towards the source and $G(\mathbf{r}, \mathbf{r}_0)$ is the acoustic Green's function [45] representing the effect at $\mathbf{r}_0$ of a point force at $\mathbf{r}$. From scattering from surfaces of finite dimensions, the free-space Green's function can be used:

$$G(\mathbf{r},\mathbf{r}_0) = \frac{\exp(ik|\mathbf{r}-\mathbf{r}_0|)}{4\pi|\mathbf{r}-\mathbf{r}_0|} \tag{18}$$

where $\mathbf{r}_0$ is on the scattering surface and $\mathbf{r}$ is some distance from the scatterer.

When the surface $\mathbf{S}_0$ is closed then the scattered field, $\psi_s(\mathbf{r}_0)$, appearing in the integrand in equation (17) is interchangeable with the total field, $\psi(\mathbf{r}_0)$. (When the scatterer is a rough surface it is often true that the surface is not closed. However, the surface may always be closed for mathematical purposes with the aid of a hypothetical surface obeying appropriate boundary conditions.) The field scattered from a surface may therefore be written as

$$\begin{aligned} \psi_s(\mathbf{r}) &= \psi(\mathbf{r}) - \psi_i(\mathbf{r}) \\ &= \int_{\mathbf{S}_0} \left[\psi(\mathbf{r}_0) \frac{\partial G(\mathbf{r},\mathbf{r}_0)}{\partial \mathbf{n}_0} - G(\mathbf{r},\mathbf{r}_0) \frac{\partial \psi(\mathbf{r}_0)}{\partial \mathbf{n}_0} \right] d\mathbf{S}_0 \end{aligned} \tag{19}$$

For scattering from rough surfaces the accuracy of the theory is affected by both the shape and dimensions of the mean surface and by the roughness of the surface. The accuracy of Kirchhoff theory is considered in section 4.5, along with the other approaches to rough surface scattering that are dealt with in the following section.

4.4 Perturbation Theories

If a rough surface deviates only slightly from a reference surface and has sufficiently small slopes, the scattered field can be calculated (approximately) using the 'method of small perturbation' (MSP) [42]. The total field in the presence of a scatterer may be written as the sum of the incident field, $\psi_i(\mathbf{r})$, and the scattered field, $\psi_s(\mathbf{r})$, as given by equation (16), above. The fields themselves may be taken to represent the displacement (or velocity) potential.

The surface height function, $h_s(x, y)$, must satisfy the following restrictions for perturbation theory to be used in the study of wave scattering:

$$\begin{aligned} k\left|h_s(x,y)\right| &<< 1 \\ \left|\nabla h_s(x,y)\right| &<< 1 \end{aligned} \tag{20}$$

The first of these restrictions arises from assuming that quantities that are functions of the surface height may be expanded as a Taylor series about their value on the mean scattering surface. Formulation of perturbation theory almost always assumes that this mean scattering surface is a plane. If the mean plane is taken to be the $z = 0$ then the Taylor expansion becomes

$$f(x,y,h_s) = f(x,y,0) + h_s \frac{\partial f(x,y,0)}{\partial z} + \frac{h_s^2}{2} \frac{\partial^2 f(x,y,0)}{\partial z^2} + \ldots \tag{21}$$

If the boundary condition on the surface of the scatterer is known, equation (21) may be used to derive an approximate boundary condition on the mean plane, $z = 0$. This gives an expression for the unknown scattered field on the mean plane in terms of known quantities. An integral formula may then be used to give the scattered field at some distance from the scatterer in terms of an integral over the mean surface of the scatterer. Therefore, the formulation of perturbation theory depends on the boundary condition satisfied at the scattering surface.

Rayleigh was the first to use the MSP in his work on the scattering of sound at sinusoidally-corrugated rough surfaces [42]. The basic principle of the method is to write the unknown scattered field as a sum of outgoing plane waves and to determine the unknown coefficients in this sum by satisfying the boundary conditions on the surface. The main restrictions are that no multiple scattering effects are included, owing to the assumption of only outgoing scattered waves, and that series convergence is only achievable if the surfaces are 'slightly rough'.

Rayleigh theory is found to be good in the limit of corrugations that are shallow compared with the incident wavelength which is a wider range of validity than perturbation theory.

4.5 Summary for scattering theory

Kirchhoff theory is exact for surfaces that are infinite, smooth and planar. For all other scatterers it is an approximation. Kirchhoff theory is valid for Gaussian surfaces when $\lambda_0 > \lambda$ and angles of incidence and scattering are small enough to ensure that grazing of the surface does not occur. Non-Gaussian surface statistics lead to reductions in the regimes of validity of this theory.

The accuracy of perturbation theory depends on the validity of the restrictions given by equation (20) and the order of terms retained in the expansion. First-order perturbation theory is usually accurate when $k\sigma_h << 1$. An additional restriction, $k\lambda_0 \leq 1$, is needed for scattering angles away from specular for Gaussian surfaces, as second-order terms may not be small compared with first-order terms.

Perturbation theory does take some account of multiple scattering effects, to an extent dependent on the order of the theory. However other effects, such as shadowing, combine to reduce the accuracy of the perturbation approach. These effects become more marked as the angles of incidence and scattering increase away from the mean surface normal (*i.e.*, shallower grazing angles).

The following section describes a number of measurements made by other researchers that have shown anomalous acoustic penetration into water-saturated sediments at sub-critical grazing angles. These researchers have proposed the use of the Biot model as a means of describing the phenomenon. However, there is some debate in academic

circles as to whether this use of the Biot model is valid. Other authors have used rough surface scattering models in an attempt to describe the phenomenon. The applicability of the different approaches to modelling rough surfaces, which have been described in this section, are considered in section 5.

5 Anomalous Acoustic Penetration

It is generally accepted that at sub-critical grazing angles and for sufficiently high frequencies only evanescent waves are transmitted into the seabed, and these cannot penetrate to any significant depth [46]. This behaviour is consistent with elastic models of acoustic propagation which are widely recognised as being applicable to propagation in sandy sediments (although there are relatively few measurements in the literature to support this).

In a series of experiments, however, Chotiros observed the transmission of acoustic energy in the 10 - 100 kHz frequency band at grazing angles less than the critical angle [1]. He conducted two field experiments and a laboratory experiment[4] over water-saturated, unconsolidated sandy sediments. Above the critical grazing angles, it was stated that compressional wave speeds were in the region of 1 700 m s^{-1}, the normally accepted value in water-saturated sand. (In the two field experiments, the measured wave speeds were found to be 1 743 m s^{-1} ± 300 m s^{-1} and 1 729 m s^{-1} ± 200 m s^{-1}. In the laboratory experiment, a wave speed of 1 675 m s^{-1} was measured, although no estimate of the associated error was provided).

In contrast, it was stated that compressional wave speeds were measured to be in the region of 1 200 m s^{-1} at sub-critical grazing angles. Also, the directions of wave propagation within the sediment were consistent with Snell's law of refraction for the speeds observed. Unfortunately, Chotiros did not provide any estimates of the errors associated with the measurements obtained at either of the two field sites or in the laboratory. This makes it difficult to compare his results with those of other authors.

---

[4] Chotiros' laboratory tank contained a 1 m thick layer of riverbed sand under a 3 m water column. An array of sensors was buried in the sand to detect acoustic signals and an omni-directional projector was suspended from a motorised platform at a height of 0.5 m above the sand. Chotiros stated that short, 60 kHz pulses were transmitted by the projector, and the acoustic signal at each sensor was recorded.

Since Chotiros' original observations, anomalous acoustic penetration of the seabed has been reported in a separate study [47]. Two possible explanations for the phenomenon have been proposed: the existence of a Biot slow wave in the bottom [48]; and forward-scattering at the rough seawater-sediment interface [49]. Chotiros has advocated the Biot slow wave although his calculations, which were based on the formulation of Stern *et al.* [50], required some radical changes to previously accepted parameters in order to match the observations.

The Biot parameters for a range of water-saturated sandy sediments have been obtained from results published by other researchers. These, and the parameters determined by Chotiros from the results of his laboratory experiment, have been evaluated to obtain a range of values for fast, slow, and shear wave speeds. This evaluation was performed using a freely-available computer program, which is described below.

A number of issues related to the use of the Biot model have been raised by other researchers. These are discussed later in this section, along with the possibility that a roughness scattering model would be more appropriate.

Schmidt developed the SAFARI computer program (Seismo-Acoustic Fast-field Algorithm for Range-Independent environments), for modelling seismo-acoustic propagation in horizontally-stratified isovelocity fluids and isotropic elastic media [51]. SAFARI can also model scattering from rough elastic interfaces using first-order perturbation theory. Later versions of the program were given the name OASES (Ocean Acoustics and Seismic Exploration Synthesis) [52]. As well as having improved numerical efficiency, the OASES program is capable of modelling acoustic propagation in poro-elastic layers, as described by the Biot theory [53]. In principle, therefore, OASES should be capable of predicting the acoustic behaviour of a wide range of sediment types, provided that the parameters input to the model have been determined correctly.

Biot parameters (porosity, grain density, *etc*., as summarised in table 1) have been determined for a range of naturally-occurring water-saturated sandy sediments in a number of separate studies. The parameters determined in five of these studies [12, 25, 50, 54, 55] are listed in table 2. In each case, values for compressional and shear

wave speeds as functions of frequency were determined from the corresponding Biot parameters using the Biot equations (as described in section 3).

Chotiros determined three sets of Biot parameters for the sediments corresponding to the field and laboratory experiments described in [1]. (The ways in which he derived some of these parameters have been subject to discussion by other authors. This is commented upon further, below). The parameters he determined for the sediment used in his laboratory experiment are also listed in table 2. He then used the Biot equations to evaluate fast, slow and shear phase speeds from his own parameters, and compared them with the speeds obtained from the five studies noted above.

	Units	**Stoll and Kan [12]**	**Hovem and Ingram [25]**	**Stern *et al* [50]**	**Ogushwitz [54]**	**Turgut *et al* [55]**	**Chotiros [1]**
Porosity	…	0.47	0.36	0.47	0.383	0.40	0.40
Grain density	kg m^{-3}	2650	2650	2650	2650	2650	2650
Liquid density	kg m^{-3}	1000	1000	1000	1000	1000	1000
Grain bulk modulus	Pa	3.60×10^{10}	3.60×10^{10}	3.60×10^{10}	4.00×10^{10}	3.60×10^{10}	7.00×10^{9}
Liquid bulk modulus	Pa	2.00×10^{9}	2.25×10^{9}	2.00×10^{9}	2.25×10^{9}	2.30×10^{9}	2.25×10^{9}
Permeability	kg m^{-1} s	1.00×10^{-10}	1.01×10^{-10}	1.00×10^{-10}	6.49×10^{-12}	1.00×10^{-11}	4.99×10^{-11}
Viscosity	m^2	1.00×10^{-3}	1.00×10^{-3}	1.00×10^{-3}	1.00×10^{-3}	1.00×10^{-3}	1.00×10^{-3}
Pore size	m	1.00×10^{-5}	3.07×10^{-5}	1.00×10^{-5}	1.84×10^{-5}	5.00×10^{-5}	4.99×10^{-5}
Structure factor	…	1.25	1.00	1.25	1.62	1.25	1.75
Frame shear modulus	Pa	2.61×10^{7}	1.00×10^{8}	2.61×10^{7}	1.19×10^{8}	5.00×10^{7}	2.61×10^{7}
Shear log decrement	…	0.15	0.00	0.15	0.10	0.063	0.15
Frame bulk modulus	Pa	4.36×10^{7}	1.00×10^{8}	4.36×10^{8}	1.99×10^{8}	1.08×10^{8}	5.30×10^{9}
Bulk log decrement	…	0.15	0.00	0.15	0.10	0.063	0.15

Table 2 *Biot model parameters that have been applied to various grades of water-saturated sandy sediments.*

In this report, the values appearing in table 2 were evaluated using the OASES program. (It is noted, above, that OASES is capable of modelling acoustic

propagation using the Biot theory). The resulting phase speeds[5] are shown in figure 2.

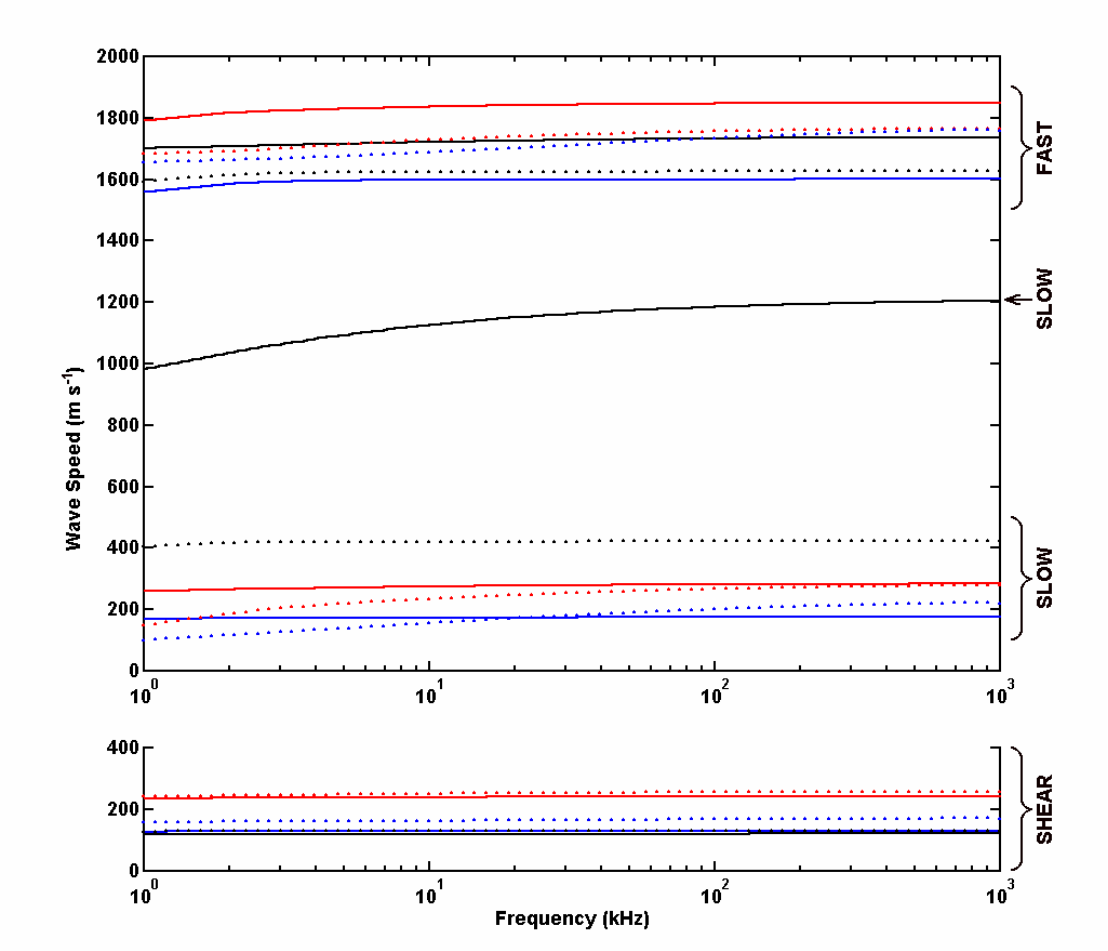

Figure 2 *Wave speeds as a function of frequency using the parameters shown in table 2 (computed using the OASES program). The curves correspond to the parameters of: Chotiros (black, solid) [1]; Stoll and Kan (blue, solid) [12]; Hovem and Ingram (red, solid) [25]; Stern et al (black, dotted) [50]; Ogushwitz (red, dotted) [54]; and Turgut and Yamamoto (blue, dotted) [55].*

It is difficult to make useful comparisons between the results in figure 2, since estimates of uncertainty were not provided by any of the authors for the parameters used in the Biot model. However, although the results from each data set are of

[5] OASES provides estimates of the complex sound speed, **c**, which is related to the complex wave number by $\mathbf{k} = \omega / \mathbf{c}$. The phase speed of a travelling wave, c_p, can be obtained from the real part of the complex wave number since $\mathbf{k} = k - ia_{np}$ and $c_p = \omega / k$ [56].

limited value when they are considered individually, it is possible to estimate valid ranges for the fast, slow and shear waves when the results are considered together.

When using the first five parameter sets in the Biot model, valid ranges of phase speeds were estimated to be between 1 550 and 1 850 m s^{-1} for the fast wave, between 100 and 400 m s^{-1} for the slow wave, and less than 300 m s^{-1} for the shear wave in the 10 - 100 kHz frequency range. The major difference exhibited by the model when using Chotiros' parameters is that the slow wave speed was predicted to be significantly higher, being around 1 200 m s^{-1} at a frequency[6] of 100 kHz.

Chotiros' model parameters are unconventional in that the grain bulk modulus is significantly lower (by a factor of 5) and the frame bulk modulus is significantly higher (by at least one order of magnitude) than in all previous estimates. Formerly it has been assumed that the grain bulk modulus of quartz sand is the same as that of quartz crystals. In contrast, Chotiros asserts that laboratory measurements have shown that sand grains are, in fact, much more compressible than quartz crystals. He also suggested that the method of calculating the frame bulk modulus from known elastic moduli, described in section 3, may be inappropriate since the equations of elastic deformation are ill-conditioned for values of Poisson's ratio close to 0.5.

The values of grain and frame bulk moduli, critical to Chotiros' results, have been examined in detail by Hickey and Sabatier [57]. They accepted that one of the major problems with the Biot theory is the difficulty in determining the necessary elastic parameters. A fundamental requirement of the theory is the assumption of an 'equivalent homogeneous solid'. For a heterogeneous matrix material, this assumption implies that the matrix will undergo the same strain as the pores in an unjacketed test [2], *i.e.*, a rock composed of the heterogeneous matrix material will behave as if it were an equivalent homogeneous rock. In modelling his observations, Chotiros used values that are incompatible with this requirement.

Further objections to the new values of grain and frame bulk moduli have been raised by Stoll [58]. He stated that, in his opinion, Chotiros was not justified in his claim that

---

[6] It has been noted that no estimates of uncertainty were available for Chotiros' parameters, which made it hard to determine the validity of the results. Many of the concerns raised in the debate surrounding Chotiros' predictions involve the validity of the assumptions made for the different Biot parameters.

a Biot slow wave with a speed of 1 200 m s^{-1} had been detected in water-saturated sand. Although the values chosen for the elastic moduli force the Biot equations to predict a slow wave speed that matched the observations, they were not representative of the material being modelled. Therefore, Stoll asserts. they should not have been used to substantiate the interpretation of field measurements.

Stoll's opinion was based on a series of calculations, including the compressional wave speed and the value of Poisson's ratio of the dry frame. The wave speed obtained from the new values was considered to be too large for any granular material confined at low effective stress levels. Also, Chotiros' value of Poisson's ratio, which was close to 0.5, was regarded as being questionable by Stoll. (Stoll noted that Poisson's ratio is usually less than about 0.2 for dry granular materials).

In his argument, Stoll made the additional point that (according to the Biot theory) the amount of energy partitioned into slow waves should have been very small, and attenuation should have been high. This is contradictory to the high amplitude of the arrival that Chotiros identified as being a slow wave.

Chotiros published a response to Stoll's criticisms [59] in which he agreed that the main issue lay with the values of the grain and frame bulk moduli. He asserted that although, historically, the frame moduli of dry and saturated sand have been assumed to be the same, the moduli values for the dry and saturated conditions are, in fact, quite different. The restricted flow of fluid between grains in the saturated condition acts to reinforce the frame, producing an increased bulk modulus. The shear modulus is also affected by the presence of the pore fluid. A similar argument was applied to the grain bulk modulus: If the frame is fluid-reinforced then a small part of the pore fluid becomes an integral part of the frame. This results in an apparent reduction of the bulk modulus of the frame material and, hence, a reduction in the operative value of the grain bulk modulus.

A second explanation for anomalous acoustic penetration, that of forward-scattering at the rough seawater-sediment interface, has also been proposed. In a recent paper by Thorsos, a rough surface approach was used in an attempt to explain the anomalous sub-critical penetration mechanism [60]. The sediment was modelled as a fluid, supporting only compressional waves. It was assumed that for sandy sediments the coupling of acoustic energy into shear waves would be negligible.

Original in colour

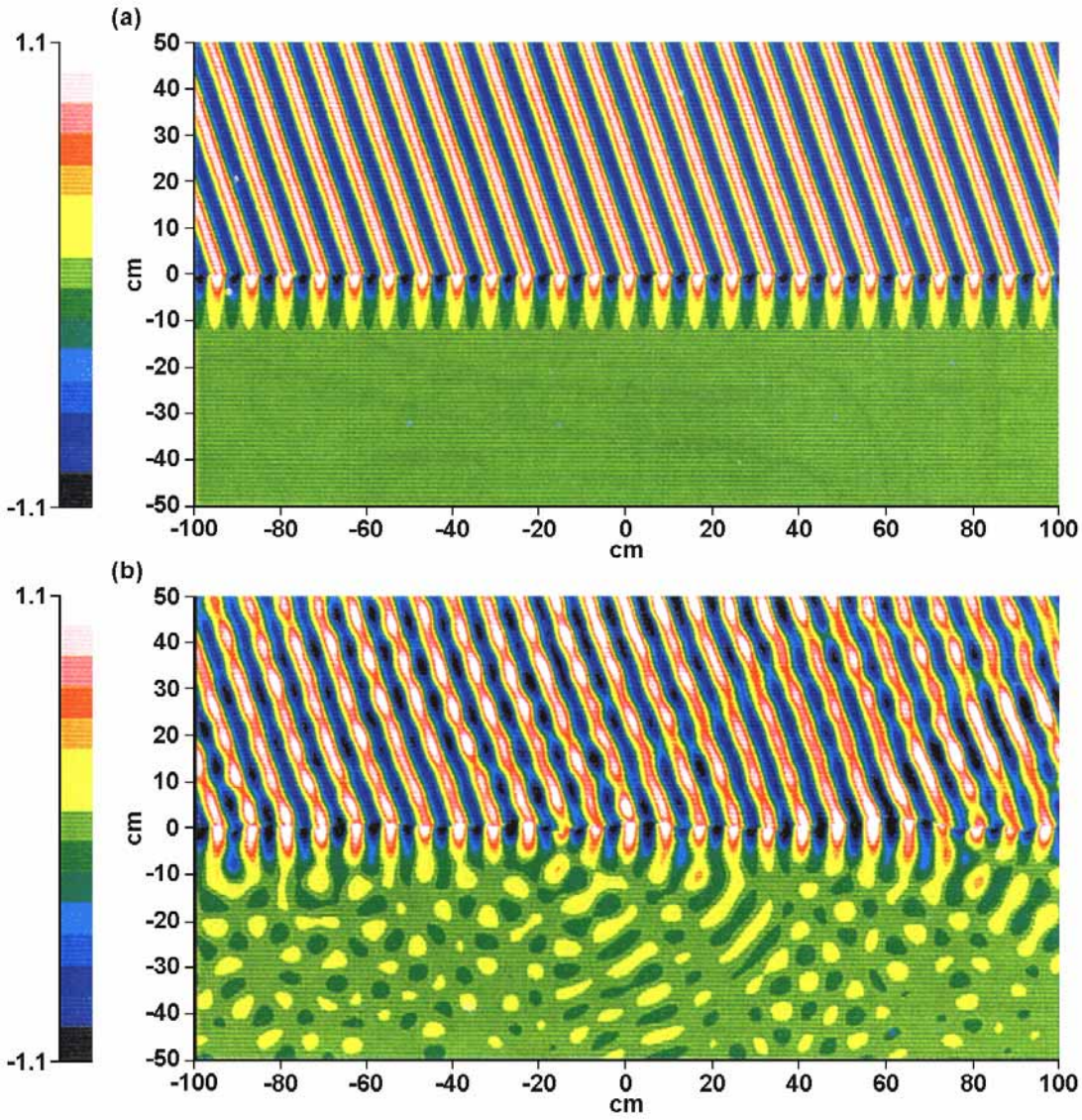

Figure 3 *Pressure fields calculated above and below a water-sediment interface using the exact integral equation method: (a) flat surface; and (b) rough surface. The incident field comes from the left at a grazing angle of 20° and the critical angle is 27.8°. (This figure was reproduced from [60] with the permission of E I Thorsos.)*

Thorsos presented a model for the penetrating field in two dimensions at a 1-D rough interface, using an exact integral equation method [32]. The speed of sound propagating in the sediment was taken to be 1 700 m s^{-1}, and roughness was defined to be $k\sigma_h = 0.66$ (where k was the acoustic wave number in the water and σ_h was the rms height of the interface). The ratio of the sound speed in the water to the sound

speed in the sediment was taken to be 1.13, which gave a critical angle of 27.8°. (In addition, the ratio of the density of the water to the density of the sediment was 2.0 and the attenuation coefficient was 0.5 dB m^{-1} kHz^{-1}).

The pressure field obtained by Thorsos using the integral equation method for both a flat and a rough surface are shown in figure 3. The mean water-sediment interface is at 0.0 cm on the vertical scale and the colour display is linear in pressure. A 20 kHz plane wave of unit magnitude is incident from the left at a grazing angle of 20°, which is well below the critical angle of 27.8°. The incident wave has been omitted to simplify the field structure.

In figure 3 (a), the surface is flat and the phase fronts of the reflected wave can be seen moving up and to the right above the interface. The field in the sediment is evanescent, *i.e.*, it decreases exponentially with depth, having a significant magnitude for only about a wavelength of depth into the sediment.

In figure 3 (b), energy can be seen to radiate down into the sediment at relatively steep angles. It is to be expected that acoustic penetration into the sediment can occur at regions along the surface where the local grazing angle exceeds the critical angle. In the simulation, however, acoustic penetration occurs even if this condition is not met anywhere on the surface.

These results show the potential for a rough interface to couple sound into the sediment at sub-critical grazing angles. To see if this mechanism could explain the acoustic penetration results reported by Chotiros, it was necessary for Thorsos to model the three-dimensional experiments. However, the integral equation approach was too computationally intensive to be extended to a full 3-D geometry. Therefore, a model based on perturbation theory was developed and used to simulate one of the two field experiments conducted by Chotiros. The model was shown to be valid for a 2-D geometry and, thus, it was expected to be valid for the 3-D geometry as well.

The surface roughness spectrum was not measured by Chotiros which made it difficult to perform a comparison between the roughness scattering model and the experimental data. Thorsos was able to estimate the roughness spectrum from data obtained in the same region at an earlier time. Acoustic waves were observed to propagate in the sediment with speeds in the 1 200 - 1 500 m s^{-1} range, depending on

the form of the spectrum. (The actual wave speed was 1 700 m s^{-1} in every case. The lower wave speeds were measured in the *apparent* direction of propagation of acoustic waves. The speed differences were the result of a purely geometrical effect).

It was also noted that, with an appropriate selection of hydrophones from the buried sensor array, the acoustic wave attenuation could be made to fit Chotiros observed attenuation of around 30 - 40 dB m^{-1} at 20 kHz. This result required that the analysis was restricted to a sub-set of the hydrophones closest to the water-sediment interface, *i.e.*, near to the evanescent wave zone.

Thorsos concluded that scattering from a rough water-sediment interface was a viable hypothesis for sub-critical penetration into sediments. In his opinion, however, further experiments were necessary to clarify whether the observed sub-critical penetration was due to the Biot slow wave mechanism, the interface roughness mechanism, or some other mechanism entirely.

6 Summary

In this report, a brief historical overview of sediment propagation models has been presented. Two theories have been covered: the Biot-Stoll theory (see section 3); and wave scattering from random rough surfaces (see section 4). The current debate surrounding the observations of, so-called, anomalous acoustic penetration has also been discussed (see section 5).

The next report in this series[3] discusses the detection of buried objects, with the apparatus arranged as described in section 4 of the second report in the series[2], and with the sediment surface being nominally smooth (*i.e.*, having an rms height of < 1 mm). Recall that, according to the Rayleigh criterion (see section 4.1), the interface appears rougher at higher grazing angles. (Although, as noted by Thorsos [60], the small difference in wave speeds between the water and sediment tends to reduce the apparent roughness of the surface for the transmission problem). Therefore the higher-angle arrangement, described in section 4 of the second report in the series[2], will 'see' a rougher sediment surface than was the case for the smooth surface in the experimental results associated with this report (see figure 8 of reference [61]).

The results presented in this current report and the associated paper [61] indicate that the signal processing system, described in a subsequent report[3], must be robust enough to cope with high levels of clutter in the received signals. Similarly, the apparent increase in the background noise level, observed in Figure 9 of reference [61], means that the detection system must also be insensitive to increased levels of background noise.

This material formed the basis of the PhD of RCPE [62-65].

References

[1] Chotiros N P, "Biot model of sound propagation in water-saturated sand", *Journal of the Acoustical Society of America*, Volume 97, Number 1, pp. 199 - 214, January 1995.

[2] Stoll R D, *Sediment Acoustics*, Springer-Verlag, 1989.

[3] Kibblewhite A C, "Attenuation of sound in marine sediments: A review with emphasis on new low-frequency data", *Journal of the Acoustical Society of America*, Volume 86, Number 2, pp. 716 - 738, August 1989.

[4] Hamilton E L, "Elastic Properties of Marine Sediments", *Journal of Geophysical Research*, Volume 76, Number 2, pp. 579 - 604, January 10, 1971.

[5] Buckingham M J, "Theory of acoustic attenuation, dispersion and pulse propagation in granular materials including marine sediments", *J. Acoust. Soc. Am.*, Vol. 102, pp. 2579 - 2596 (1997).

[6] Buckingham M J, "Seismic Wave Propagation in Rocks and Marine Sediments: A New Theoretical Approach", *Proceedings of the Fourth European Conference on Underwater Acoustics*, Edited by Alippi A and Cannelli G B, pp. 301 - 306, Rome, 1998.

[7] Hovem J M, "Attenuation of sound in marine sediments", Electronics Research Laboratory, University of Trondheim, Norway.

[8] Urick R J, *Principles of Underwater Sound*, McGraw-Hill, New York, 3rd Edition, Section 5.8, pp. 136 - 143, 1983.

[9] Hamilton E L, "Compressional-wave attenuation in marine sediments", *Geophysics*, pp. 620 - 646, August 1972.

[10] Biot M A, "Theory of Propagation of Elastic Waves in a Fluid-Saturated Porous Solid. I. Low-Frequency Range", *Journal of the Acoustical Society of America*, Volume 28, Number 2, March 1956.

[11] Biot M A, "Theory of Propagation of Elastic Waves in a Fluid-Saturated Porous Solid. II. Higher Frequency Range", *Journal of the Acoustical Society of America*, Volume 28, Number 2, March 1956.

[12] Stoll R D, Kan T -K, "Reflection of acoustic waves at a water-sediment interface", *Journal of the Acoustical Society of America*, Volume 70, Number 1, pp. 149 - 156, July 1981.

[13] Stoll R D, "Marine sediment acoustics", *Journal of the Acoustical Society of America*, Volume 77, Number 5, pp. 1789 - 1799, May 1985.

[14] Boyle F A, Chotiros N P, "A model for acoustic backscatter from muddy sediments", *Journal of the Acoustical Society of America*, Volume 98, Number 1, pp. 525 - 530, July 1995.

[15] Buckingham M J, "Theory of compressional and shear waves in fluidlike marine sediments", *J. Acoust. Soc. Am.*, Vol. 103, No. 1, pp. 288 - 299 (1998).

[16] Brekhovskikh L M, Lysanov Y P, *Fundamentals of Ocean Acoustics*, Second Edition, Chapter 3, Springer-Verlag, 1991.

[17] Buckingham M J, "On the phase speed and attenuation of an interface wave in an unconsolidated marine sediment", *Journal of the Acoustical Society of America*, Volume 106, Number 4, pp. 1694-1703, October 1999.

[18] Brekhovskikh L M, *Waves in Layered Media*, 2nd Edition, Chapter 1, pp. 48 - 50, Academic Press, 1980.

[19] Boyle F A, Chotiros N P, "A model for high-frequency acoustic backscatter from gas bubbles in sandy sediments at shallow grazing angles", *Journal of the Acoustical Society of America*, Volume 98, Number 1, pp. 531 - 541, July 1995.

[20] Boyle F A, Chotiros N P, "Nonlinear acoustic scattering from a gassy poroelastic seabed", *Journal of the Acoustical Society of America*, Volume 103, Number 3, pp. 1328 - 1336, March 1998.

[21] Holland C W, Brunson B A, "The Biot-Stoll sediment model: An experimental assessment", *Journal of the Acoustical Society of America*, Volume 84, Number 4, pp. 1437 - 1443, October 1988.

[22] Hamilton E L, "Sound attenuation as a function of depth in the sea floor", *J. Acoust. Soc. Am.*, Vol. 59, No. 3, pp. 528-535, March 1976.

[23] Hamilton E L, "Acoustic Properties of Sediments", *Acoustics and Ocean Bottom*, edited by A. Lara-Saenz, C. Ranz Guerra, and C. Carbofite Consejo Superior de Investigaciones Cientificas (CSIC), Madrid (1987).

[24] Carman P C, *Flow of Gases through Porous Media*, Academic Press, New York, 1956.

[25] Hovem J M, Ingram G D, "Viscous attenuation of sound in saturated sand", *Journal of the Acoustical Society of America*, Volume 66, Number 6, pp. 1807 - 1812, December, 1979.

[26] Patterson R E, "Backscatter of sound from a rough boundary", *Journal of the Acoustical Society of America*, Volume 35, pp. 2010 - 2013, 1963.

[27] Clay C S, Medwin H, *Acoustical Oceanography: Principles and Applications*, John Wiley & Sons, New York, 1977.

[28] McDaniel S T, Gorman A D, "An examination of the composite roughness scattering model", *Journal of the Acoustical Society of America*, Volume73, pp. 1476 - 1486, 1983.

[29] Jackson D R, Winebrenner D P, Ishimaru A, "Application of the composite roughness scattering model", *Journal of the Acoustical Society of America*, Volume 79, pp. 1410 - 1422, 1986.

[30] Thorsos E I, “An investigation of the small slope approximation for scattering from rough surfaces. Part I. Theory”, *Journal of the Acoustical Society of America*, Volume 97, Number 4, pp. 2082 - 2093, April 1995.

[31] Urick R J, “Side scattering of sound in shallow water”, *Journal of the Acoustical Society of America*, Volume 32, pp. 351 - 355, 1960.

[32] Ivakin A N, “A unified approach to volume and roughness scattering”, *Journal of the Acoustical Society of America*, Volume 103, Number 2, pp. 827 - 837, February 1998.

[33] Jackson D R, Briggs K B, “High-frequency bottom backscattering: Roughness versus interface scattering”, *Journal of the Acoustical Society of America*, Volume 92, pp. 962 - 977, 1992.

[34] Jackson D R, Ivakin A N, “Scattering from elastic sea beds: First-order theory”, *Journal of the Acoustical Society of America*, Volume 103, Number 1, pp. 336 - 345, January 1998.

[35] Ogilvy J A, *Theory of Wave Scattering from Random Rough Surfaces*, Adam Hilger, Bristol, 1991.

[36] Bradley C R, Stephen R A, “Modeling of seafloor wave propagation and acoustic scattering in 3-D heterogeneous media”, *Journal of the Acoustical Society of America*, Volume 100, Number 1, pp. 225 - 236, July 1996.

[37] McLane M, *Sedimentology*, Chapter 5, p. 88, Oxford University Press, Inc., 1995.

[38] Pinet P R, *Oceanography: An Introduction to the Planet Oceanus*, Chapter 4, p. 106, West Publishing Company, 1992.

[39] McLane M, *Sedimentology*, Chapter 2, p. 14, Oxford University Press, Inc., 1995.

[40] Pace N G, Ceen R V, “Transient Parametric Arrays Terminated at a Water/Sediment Interface”, *Acoustics and the Sea-Bed,* Conference Proceedings (Institute of Acoustics, Underwater Acoustics Group), pp. 411 – 422, Bath University Press, UK, 1983.

[41] Brekhovskikh L M, Lysanov Y P, *Fundamentals of Ocean Acoustics*, Second Edition, Section 9.1, Springer-Verlag, 1991.

[42] Brekhovskikh L M, Lysanov Y P, *Fundamentals of Ocean Acoustics*, Second Edition, Section 9.2, Springer-Verlag, 1991.

[43] Goff J A, Jordan T H, “Stochastic Modeling of Seafloor Morphology: Inversion of Sea Beam Data for Second-Order Statistics”, *J. Geophys. Res.*, Vol. 93, No. B11, pp. 13589 - 13608, November 10, 1988.

[44] Brekhovskikh L M, Lysanov Y P, *Fundamentals of Ocean Acoustics*, Second Edition, Section 9.7, Springer-Verlag, 1991.

[45] Nelson P A, “An introduction to acoustics”, pp. 50 - 56 (Fahy F, Walker J, *Fundamentals of Noise and Vibration*, E & FN Spon, London and New York, 1998).

[46] Pain H J, *The Physics of Vibrations and Waves*, 4th Edition, John Wiley & Sons Ltd, pp. 235 - 240, 1995.

[47] Lopes J L, “Observations of anomalous acoustic penetration into sediments at shallow grazing angles”, *J. Acoust. Soc. Am.*, Vol. 99, Number 4, pp. 2473 - 2500, April 1996.

[48] Chotiros N P, “Acoustic penetration of ocean sediments in the context of Biot's theory”, *J. Acoust. Soc. Am.*, Vol. 99, Number 4, pp. 2474 - 2500, April 1996.

[49] Jackson D R, Moe J E, Thorsos E I, Williams K L, "Subcritical penetration of sandy sediments due to interface roughness", *J. Acoust. Soc. Am.*, Vol. 99, Number 4, pp. 2474 - 2500, April 1996.

[50] Stern M, Bedford A, Millwater H R, "Wave reflection from a sediment layer with depth-dependent properties", *Journal of the Acoustical Society of America*, Volume 77, Number 5, pp. 1781 - 1788, May 1985.

[51] Schmidt H, *SAFARI User's Guide*, SACLANTCEN Report, Serial Number SR-113, SACLANT Undersea Research Centre, Italy, 1988.

[52] Schmidt H, *OASES Version 2.1 User Guide and Reference Manual*, Dept. Ocean Eng., MIT, August 1997.

[53] Schmidt H, Lee J, Fan H, LePage K, "Multi-static bottom reverberation in shallow water", SACLANTCEN Conference Proceedings CP-45, NATO SACLANT Undersea Research Centre, pp. 475 - 482, 1997.

[54] Ogushwitz P R, "Applicability of the Biot theory, III. Wave speeds versus depth in marine sediments", *J. Acoust. Soc. Am.*, Volume 77, pp. 453 - 464, 1985.

[55] Turgut A, Yamamoto T, "Measurements of acoustic wave velocities and attenuation in marine sediments", *J. Acoust. Soc. Am.*, Volume 87, pp. 2376 - 2382, 1990.

[56] Kinsler L E, Frey A R, Coppens A B, Sanders J V, *Fundamentals of Acoustics*, 3rd Edition, John Wiley & Sons, Inc, Toronto, Chapter 5, pp. 142 - 146, 1982.

[57] Hickey C J, Sabatier J M, "Choosing Biot parameters for modeling water-saturated sand", *Journal of the Acoustical Society of America*, Volume 102, Number 3, pp. 1480 - 1484, September 1997.

[58] Stoll R D, "Comments on 'Biot model of sound propagation in water-saturated sand' J. Acoust. Soc. Am. 97, 199-214 (1995)", *Journal of the Acoustical Society of America*, Volume 103, Number 5, Part 1, pp. 2723 - 2725, May 1998.

[59] Chotiros N P, "Response to: 'Comments on 'Biot model of sound propagation in water-saturated sand'' J. Acoust. Soc. Am. 97, 199-214 (1995)", *Journal of the Acoustical Society of America*, Volume 103, Number 5, Part 1, pp. 2726 - 2729, May 1998.

[60] Thorsos E I, Jackson D R, Moe J E, Williams K L, "Modeling of Subcritical Penetration into Sediments Due to Interface Roughness", SACLANTCEN Conference Proceedings CP-45, NATO SACLANT Undersea Research Centre, pp. 563 - 569, 1997.

[61] T G Leighton and R C P Evans, The detection by sonar of difficult targets (including centimetre-scale plastic objects and optical fibres) buried in saturated sediment, *Applied Acoustics* 2007 (in press).

[62] Evans, R C P, "Acoustic penetration of the seabed, with particular application to the detection of non-metallic buried cables", *PhD Thesis, University of Southampton,* 1999.

[63] Evans R C. Leighton T G, "The Detection of cylindrical objects of low acoustic contrast buried in the seabed", *J. Acoust. Soc. Am.*, Vol. 103, p. 2902, 1998.

[64] Evans R C,. Leighton T G, "The Detection of Cylindrical Objects of Low Acoustic Contrast Buried in the Seabed", *Proceedings of the 16th International Congress on Acoustics and 135th*

Meeting of the Acoustical Society of America (ICA/ASA '98), Edited by Kuhl P K and Crum L A, pp. 1369 - 1370, 1998.

[65] Evans R C, Leighton T G, "An experimental investigation of acoustic penetration into sandy sediments at sub-critical grazing angles", *Proceedings of the Fourth European Conference on Underwater Acoustics*, Edited by Alippi A and Cannelli G B, pp. 697 - 702, 1998.